OMICS A Journal of Integrative Biology
Volume 27, Number 7, 2023

DOI: 10.1089/omi.2023.0066

Idiopathic Pulmonary Arterial Hypertension: Network-Based Integration of Multi-Omics Data Reveals New Molecular Signatures and Candidate Drugs

Ceyda Kasavi

Abstract

Idiopathic pulmonary arterial hypertension (IPAH) is a progressive disease that affects the pulmonary arteries, resulting in increased pulmonary vascular resistance and right ventricular dysfunction, which can ultimately lead to heart failure and death. The molecular substrates of IPAH are poorly understood while diagnostics and therapeutics innovation remain as unmet needs for this debilitating disease. In this study, a network-based methodology was used to uncover the salient molecular mechanisms of IPAH to inform drug and diagnostic discovery, and personalized medicine. Expression profiling datasets associated with IPAH were obtained from the Gene Expression Omnibus database: GSE15197, GSE113439, GSE53408, and GSE67597. The comparative analysis of mRNA and miRNA expression data and the modular analysis of a transcriptome-based weighted gene coexpression network unraveled disease-specific gene and miRNA signatures. DEAD-box helicase 52 (*DDx52*), ESF1 nucleolar pre-RNA processing protein (*ESF1*), heterogeneous nuclear ribonuclearprotein A3 (*MNRNPA3*), Myosin VA (*MYO5A*), replication factor C subunit 1 (*RFC1*), and arginine and serine rich coiled coil 1 (*RSRC1*) were detected as the salient genes for IPAH. In addition, the salient gene-based drug repositioning analysis identified alvespimycin, tanespimycin, geldanamycin, LY294002, cephaeline, digoxigenin, lanatoside C, helveticoside, trichostatin A, phenoxybenzamine, genistein, pioglitazone, and rosiglitazone as potential drug candidates for IPAH. In conclusion, this study provides new molecular signatures in relation to IPAH and attendant potential drug candidates for further experimental and translational clinical research for patients with IPAH.

Keywords: pulmonary arterial hypertension, biomarker, drugs, omics, protein–protein interaction, lung disease

Introduction

IDIOPATHIC PULMONARY ARTERIAL HYPERTENSION (IPAH) is a chronic and progressive disease characterized by elevated pulmonary artery pressure leading to right heart failure and death (Schlueter et al., 2020; Swaminathan et al., 2020). An increase in the mean pulmonary artery pressure >25 mmHg at rest, a pulmonary vascular resistance of greater than three Wood units, and a pulmonary capillary wedge pressure of <15 mmHg at end expiration are used to identify the disease (Luo et al., 2020). IPAH is the sporadic form of pulmonary arterial hypertension while familial form of the disease caused by inherited genetic mutations also exists as well as secondary forms owing to drugs and connective tissue disease (Rajkumar et al., 2010; Zhao et al., 2014).

The prevalence of pulmonary arterial hypertension (PAH) and IPAH is 15 and 5.9 cases per million adult population, respectively, according to the 2015 European Society of Cardiology/European Respiratory Society (ESC/ERS) guidelines (Galiè et al., 2015). Hendriks et al. reported a 5- and 10-year transplant-free survival rates of 71% and 35%, respectively. Despite advances in treatment strategies, the survival rate for incident patients still remains unsatisfactory (Hendriks et al., 2022).

The pathophysiological changes associated with PAH are diverse and complex. Several genetic, epigenetic, and environmental factors contribute to its progression. Proliferative remodeling, endothelial cell dysfunction, fibrosis, and inflammation are among the main pathological hallmarks of PAH (Li et al., 2020; Mayeux et al., 2021). PAH also exhibits

Department of Bioengineering, Faculty of Engineering, Marmara University, Istanbul, Turkey.

cancer-like biological features such as cell proliferation, angiogenesis, and resistance to apoptosis of fibroblasts, pulmonary artery smooth muscle cells, and pulmonary artery endothelial cells (Boucherat et al., 2017; Wu et al., 2016; Zeng et al., 2021).

Although the impact of PAH has been widely reported, its pathogenesis is still not fully understood (Li et al., 2020). Therefore, the elucidation of the molecular mechanisms underlying PAH would improve our understanding of the disease pathogenesis and provide valuable information for the discovery and development of predictive biomarkers.

Therapeutic options for patients with PAH have gradually evolved over the past decade. Treatment strategies aim to improve patients' quality of life, exercise capacity and right ventricular function, and reduce the risk of mortality (Galiè et al., 2015). Medical management includes drugs that target pathways associated with disease progression, such as the nitric oxide, endothelin-1, and prostacyclin pathways (Mayeux et al., 2021). The beneficial effects of anticancer drugs in combination with vasodilators have also been investigated (Boucherat et al., 2017). Current therapies can alleviate PAH by reducing the pulmonary vascular resistance, but no effective drug therapy has been developed to completely reverse the vascular remodeling of the pulmonary arteries (Galiè et al., 2015; Li et al., 2020). Therefore, new approaches for the discovery of molecular targets and drug candidates are needed.

The development of omics technologies enables system-level network analysis to unravel the molecular mechanisms behind human diseases and to identify novel biomarker candidates for therapeutic purposes. A multi-omics approach to PAH may lead to the identification of new diagnostic and therapeutic targets and improve treatment efficacy.

Weighted gene coexpression network analysis (WGCNA) identifies highly correlated gene modules, determines modules significantly associated with sample traits, and identifies hub genes using module-to-module and gene-to-module relationship measures (Langfelder and Horvath, 2008). Application of WGCNA to various human diseases has led to the identification of important molecular targets for treatment and therapeutic purposes (Auwul et al., 2021; Brohawn et al., 2016; Yan, 2018; Zhang et al., 2018a).

In this study, an integrative analysis of genome-wide gene and miRNA expression data from patients with IPAH and controls was performed to identify molecular signatures and repositioned drug candidates for therapeutic purposes. Specifically, differentially expressed genes (DEGs), miRNAs (DEmiRNAs), and their associations were identified. In addition, a gene coexpression network was constructed, and co-analyzed with human protein-protein interaction (PPI) network to identify novel molecular signatures. Following the cross-validation analysis, a drug repositioning approach was applied to determine the potential drugs that could be effective for IPAH.

Materials and Methods

Study sample, data acquisition, and analysis

Expression profiling datasets associated with IPAH were obtained from the Gene Expression Omnibus (GEO) database (Barrett and Edgar, 2006) at the National Center for Biotechnology Information.

The explore dataset GSE15197 (Rajkumar et al., 2010), which was performed based on the Agilent-014850 Whole Human Genome Microarray 4x44K G4112F platform, contained 39 lung samples from 18 patients with IPAH, 8 patients with idiopathic pulmonary fibrosis (IPF) with secondary IPAH, and 13 normal controls. As IPAH was specifically investigated in this study, the samples from IPF with secondary IPAH were excluded from that dataset.

The datasets of GSE113439 (Mura et al., 2019) and GSE53408 (Zhao et al., 2014) were downloaded for further data validation analysis. GSE113439 contains lung samples from 6 patients with IPAH and 11 normal controls; and GSE53408 contains lung samples from 5 patients with IPAH and 11 normal controls based on the Affymetrix Human Gene 1.0 ST Array platform. PAH secondary to other diseases were excluded from the validation datasets and only IPAH samples were used for further analyses. The miRNA expression profiling dataset GSE67597 (Wu et al., 2016), obtained from the Agilent-046064 Unrestricted_Human_miRNA_V19.0_ Microarray platform, consisted of lung tissues samples from 15 individuals, including 7 IPAH patients and 8 age-matched control donors.

Differential gene expression and miRNA expression analyses were performed using the GEO2R tool (www.ncbi.nlm.nih.gov/geo/geo2r/). Raw gene and miRNA expression data were normalized by quantile normalization, and DEGs and DEmiRNAs were identified using normalized expression values by Linear Models of Microarray Data (LIMMA) (Smyth, 2004). The Benjamini–Hochberg method was used to control the false discovery rate (FDR). Statistical significance and expression patterns were determined by adjusted p-value (adj. p-value) and fold-change (FC), respectively. An adjusted p-value threshold of 0.05 (adj. p-value <0.05) was maintained to identify significantly expressed genes (SEGs). Then, an FC cutoff of 2 was used to determine the regulatory pattern (up- and downregulation) of each gene to identify DEGs. A p-value threshold of 0.05 ($p < 0.05$) and an FC cutoff of 4 were used to determine the statistical significance and regulatory pattern of each miRNA, respectively.

To elucidate the association between DEmiRNAs and DEGs, experimentally validated miRNA-target gene interactions were retrieved from the miRTarbase database (Release 9.0) (Huang et al., 2022).

This article presents a computational analysis of gene expression data obtained from public databases. It does not contain any studies with human and animal subjects and therefore does not require IRB approval.

Construction of weighted gene coexpression network and selection of key modules

The weighted gene coexpression network was constructed using the WGCNA package (Langfelder and Horvath, 2008) version 1.70–3 in R software (R Core Team, 2020). The samples in the GSE15197 dataset were clustered based on the average linkage hierarchical clustering method through the hclust function, and the cluster dendrogram was constructed to check and exclude the outlier samples.

For network construction, soft-threshold power β was determined by the pickSoftThreshold function according to the standard of scale-free networks, and correlations between

all gene pairs were calculated by Pearson correlation coefficients (PCCs). First, a signed adjacency matrix was constructed using the soft-threshold power and the similarity matrix consisting of the PCCs of all gene pairs. Then, the adjacency matrix was transformed into the topological overlap matrix (TOM), and the dissimilarity matrix (dissTOM) was computed.

The coexpression modules were then determined using the dynamic branch-cutting method, with the minimum module size and deepSplit set to 30 and 2, respectively. Genes with similar expression profiles were placed in the same modules and a hierarchical clustering dendrogram of genes was constructed. Similar modules were further merged by using module eigengene (ME), which summarizes the expression profiles of each module. The dissimilarity of the MEs was calculated and the ME cut height was set to 0.25 as the module merging criterion.

Key modules that are significantly associated with clinical traits of IPAH were determined by calculating the PCCs between MEs and clinical traits. Specifically, modules that showed significant positive correlation with IPAH ($r > 0.6$, and p-value <0.01) were selected as key modules. Then, genes in key modules were prioritized based on their connectivity, and the highly connected genes were determined using two measures: gene significance (GS) and module membership (MM). GS, which shows the correlation between gene expression and clinical trait, and MM, which defines the correlation between gene expression and ME, were calculated for each gene in key modules.

Functional enrichment analyses

Functional enrichment analysis was performed using the ShinyGO (v0.76.3) enrichment tool (Kamburov et al., 2013) to identify significantly enriched Gene Ontology (GO) biological process (BP) terms and molecular pathways using the GO (Ashburner et al., 2000) and the Kyoto Encyclopedia of Genes and Genomes (KEGG) (Kanehisa and Goto, 2000) databases as annotation sources, respectively. Enrichment analysis was calculated based on the hypergeometric distribution and p-values were corrected using FDR. An FDR cutoff of 0.05 (FDR <0.05) was used to determine the statistical significance.

Reconstruction and analysis of PPI networks

PPIs between the proteins encoded by coexpressed genes were extracted from the STRING database (https://string-db.org) (Szklarczyk et al., 2021) using a confidence score of 0.7. PPI networks were reconstructed individually for each key module via Cytoscape version 3.9.1 (Shannon et al., 2003). Network modules were identified by Cytoscape's MCODE plug-in (Bader and Hogue, 2003). In MCODE, network scores were computed by excluding the loops. Modules were identified by setting the degree threshold, node score threshold, K-core threshold, and maximum depth to 2, 0.2, 2, and 100, respectively. The fluff parameter was turned off and the haircut parameter was turned on.

Determination and validation of hub genes

To increase the biological significance and to better represent the genetic characteristics of IPAH, hub genes were identified by a combined analysis of WGCNA key modules, PPI network modules, and DEGs. In a coexpressed gene module, hub genes were determined taking into account their correlation with the clinical trait and the degree of connectivity. Therefore, GS and MM values were calculated, and genes that fulfilled $|MM| > 0.8$ and $|GS| > 0.5$ in key modules were selected as WGCNA hub genes. In PPI networks, hub proteins were determined based on modularity. The genes encoding proteins in modules with at least 5 members and a minimum score of 5 were recognized as PPI hub genes. The common genes among the WGCNA hubs, PPI hubs, and DEGs of the GSE15197 dataset were selected for validation analyses.

Two independent gene expression datasets, GSE113439 and GSE53408, were used to test the validity of the common hub genes. The genes that also showed significantly altered expression in the GSE113439 and GSE53408 datasets were selected as key genes for further analysis.

Diagnostic performance analysis of key genes

Key genes were subjected to diagnostic performance analysis. Gene expression profiles of the key genes were extracted from the GSE15197 dataset, and receiver operating characteristic (ROC) curves were plotted in R. The area under the curve (AUC), which represents sensitivity (the proportion of positive test results in patients) and specificity (the proportion of negative test results in healthy individuals), was used to evaluate the diagnostic performance of the key genes. Statistical significance was determined using an AUC value threshold of 70% and genes with an AUC value ≥70% were considered as diagnostic.

Identification of candidate drugs

Drug Gene Budger (DGB) (Wang et al., 2019b), a web-based application, was searched for potential therapeutic agents targeting key genes identified in IPAH. DGB provides a list of small molecules that are predicted to affect the expression of the target gene of interest. The expression patterns (upregulation or downregulation) of target genes in response to the predicted small molecules were assessed using the log-transformed FC, p-value, and q-value for each small molecule, and the significance of differential expression was determined using the LIMMA method.

The experimental data extracted from the original Connectivity Map (Lamb et al., 2006) and GEO datasets compiled by the DGB were used to identify drugs or compounds targeting key genes. Significant drugs were selected based on a q-value threshold of 0.05 (q-value <0.05). The repositioned drugs were further investigated through L1000 fireworks display (L100FWD) (Wang et al., 2018) and Drugbank (Wishart et al., 2018) databases, and unknown drugs were eliminated.

Results

DEGs and DEmiRNAs in IPAH

The explore dataset (GSE15197) containing gene expression data from lung samples of IPAH patients and healthy controls was comparatively analyzed to identify DEGs and their expression patterns. Statistical analyses revealed 7466 SEGs based on an adj. p-value <0.05 criterion. Considering

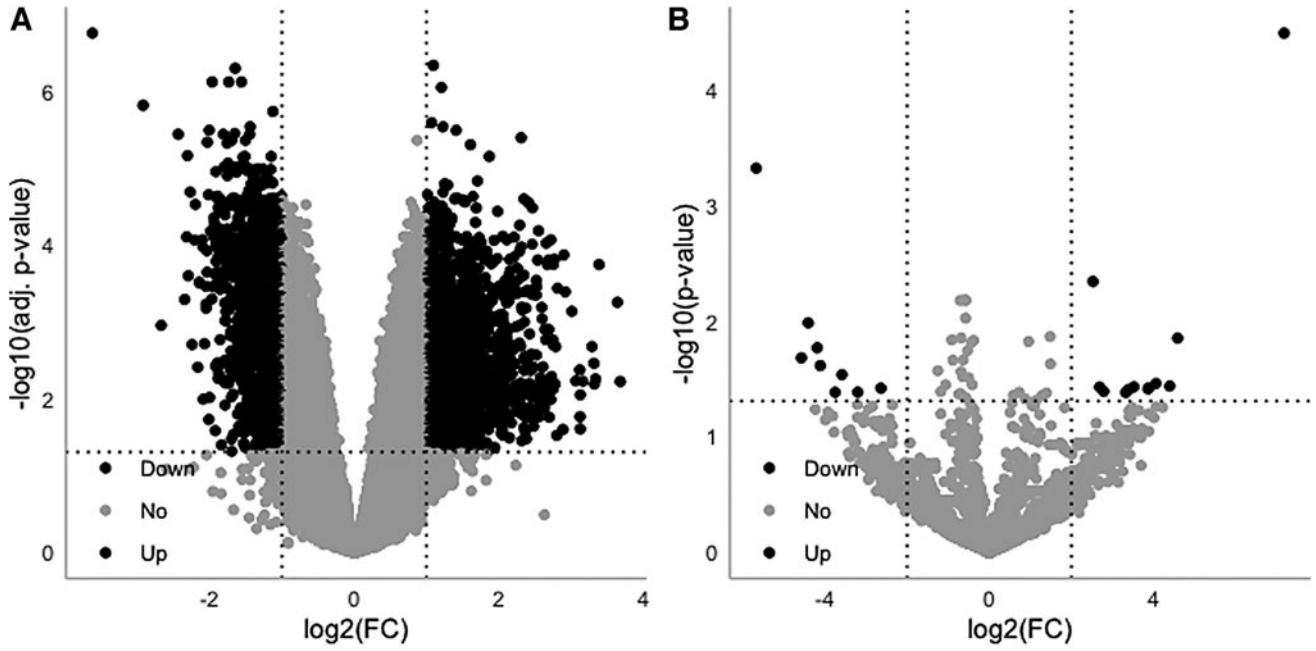

FIG. 1. **(A)** mRNA profiling **(B)** miRNA profiling by volcano plot. The x-axis represents the log2 transformed FCs; the y-axis represents the −log10 transformed *p*-values. The *dark dots* represent DEGs and DEmiRNAs. DEmiRNAs, differentially expressed miRNAs; DEGs, differentially expressed genes; FCs, fold-changes.

the FC in expression levels, a total of 2361 DEGs (1254 upregulated, 1107 downregulated) were identified (Fig. 1A).

Global miRNA expression profile analysis was performed using the GSE67597 dataset. A total of 51 miRNAs showed significantly altered expression levels in IPAH compared with controls. In addition to *p*-values, at least an 4-FC in mean expression levels was used to identify DEmiRNAs and their regulatory pattern. This analysis revealed 12 upregulated (miR-505-5p, miR-183-5p, miR-375, miR-500a-3p, miR-6074, miR-152, miR-31-5p, miR-198, miR-648, miR-4473, miR-3974, and miR-205-5p) and 9 downregulated (miR-146b-3p, miR-1256, miR-302f, miR-517a-3p, miR-4693-5p, miR-4704-3p, miR-1178-3p, miR-495-5p, and miR-1253) DEmiRNAs (Fig. 1B).

To reveal regulatory associations in disease pathogenesis, the miRNA-target gene regulatory network was reconstructed by collecting DEmiRNA-DEG interactions. The constructed network contained 423 associations between 343 DEGs and 20 DEmiRNAs (Supplementary Fig. S1). To elucidate the molecular pathways and BPs underlying IPAH, functional enrichment analysis of DEmiRNAs was performed via DEGs regulated by these DEmiRNAs (Supplementary Fig. S2).

Pathway enrichment of upregulated DEmiRNAs revealed several cancer and cancer-associated pathways, several infection-related disease pathways, MAPK signaling, HIF-1 signaling, neurotrophin signaling, sphingolipid signaling, lipid and atherosclerosis, hypertrophic and arrhythmogenic right ventricular cardiomyopathy, ferroptosis, and endocrine-related pathways such as endocrine resistance and prolactin signaling. In addition, RNA processing, neurogenesis, neuron generation, central nervous system development, glial cell development, transmembrane transport, L-glutamate and glucose transport, cell cycle, endothelial cell differentiation, vasculature development, and myocardial tissue development were identified as upregulated BPs. On the contrary, downregulated DEmiRNAs were significantly enriched only in the axon guidance pathway. This group was found to be significantly associated with processes related to heart valve development and morphogenesis, including mitral, atrioventricular, and tricuspid valves, embryonic development, cardiac ventricle development, ventricular septum development, positive regulation of oxidative stress-induced cell death, and neuronal death.

Weighted gene coexpression network

Gene coexpression network analysis was performed on 7466 SEGs from the explore dataset GSE15197. The cluster dendrogram of the samples revealed one sample (GSM379341) as an outlier (Fig. 2A). Therefore, this sample was excluded from further analysis, and 30 samples (17 IPAHs, and 13 controls) were included for WGCNA. A scale-free network was constructed with a soft-threshold power of $\beta = 20$ and $R^2 = 0.90$ (Fig. 2B). A total of 21 modules were identified (Fig. 2C). The genes with similar expression profiles were grouped into the same module, and after module merging, three coexpressed modules were obtained. The cluster dendrogram of these modules is given in Figure 2C. The magenta module containing 2753 genes was the largest module, followed by the black module (1623 genes) and the brown module (1589 genes).

All ungrouped genes that were not coexpressed were included in the gray module (1501 genes). The correlations between the coexpressed modules were presented using the ME dendrogram and heatmap (Fig. 2D).

To better understand the biological significance of coexpressed gene modules in disease progression, the correlation between MEs of major modules and clinical traits was considered (Fig. 2E). The module–trait relationship analysis showed

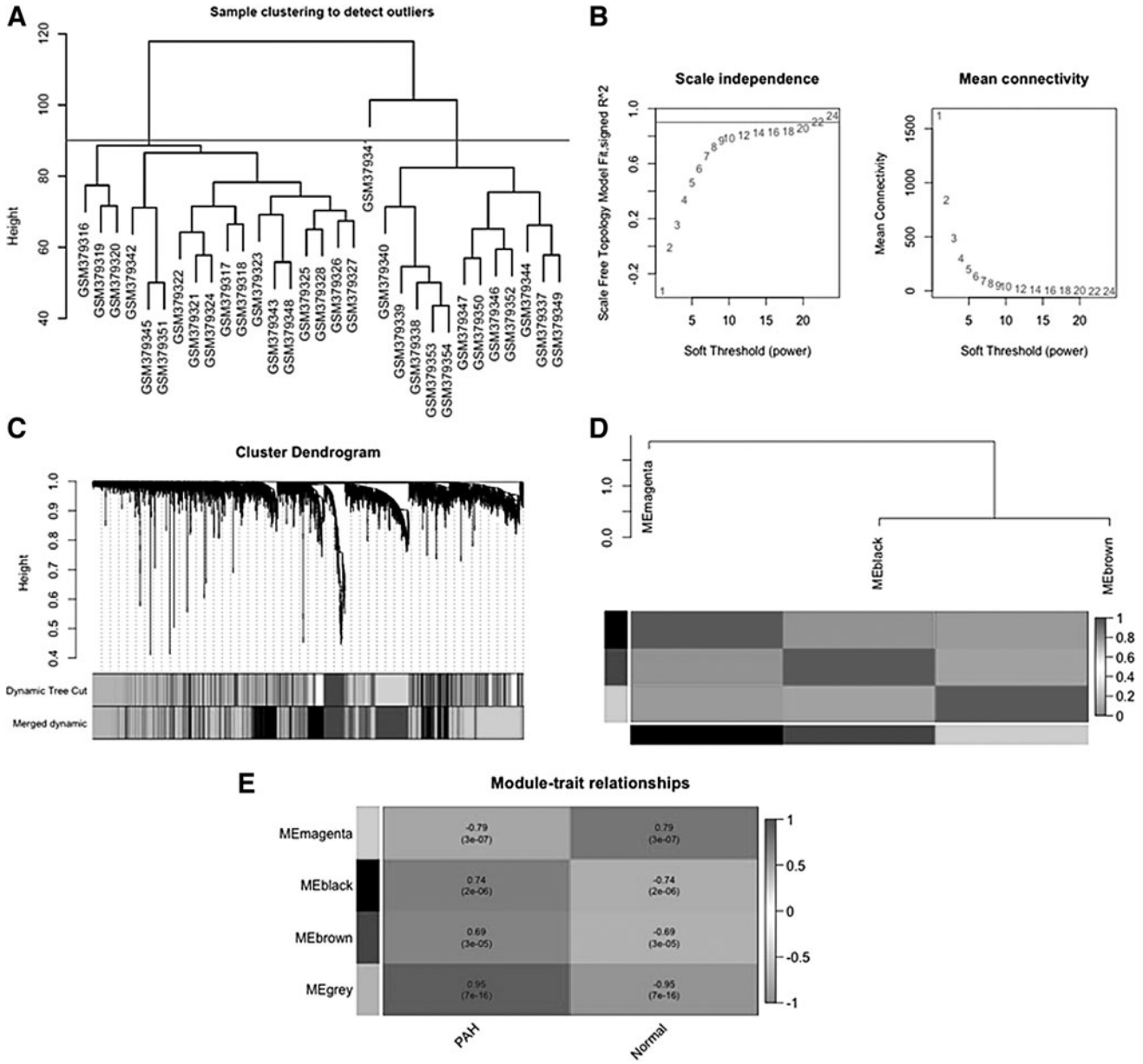

FIG. 2. Construction of the WGCNA network. **(A)** The cluster dendrogram of the samples. **(B)** Determination of the soft-threshold power β for scale-free network construction and the mean connectivity for the soft-threshold power. The coefficient threshold was set to 0.9 and the soft-threshold power was 20. **(C)** A cluster dendrogram built based on the dissimilarity matrix (1-TOM). **(D)** ME dendrogram and heat map. **(E)** Heatmap demonstrating the correlation between MEs and clinical traits. ME, module eigengene; TOM, topological overlap matrix; WGCNA, weighted gene coexpression network analysis.

that the black module ($r = 0.74$, p-value = 2E-06) and the brown module ($r = 0.69$, p-value = 3E-05) had a significant positive correlation with IPAH. Since genes in the black and brown modules may play a key role in the progression of IPAH, these modules were selected as the clinically significant key modules.

To gain further biological insight into the genes in the brown and black modules, enrichment analyses were performed, and the top 10 significantly enriched GO BP terms, and KEGG pathways are given in Figure 3.

Pathway enrichment analysis revealed that the brown module genes were mainly enriched in pathways involved in maintaining genome stability (mismatch repair, nucleotide excision repair, and spliceosome), pathways involved in protein processing (ribosome, and protein processing in endoplasmic reticulum), several cancer pathways, various infectious diseases, autophagy, HIF-1 signaling pathway, and EGFR tyrosine kinase inhibitor resistance. In addition, brown module genes were found to be significantly involved in RNA processing, chromatin organization and remodeling, histone modification, methylation, gene silencing, cell cycle, neurogenesis, brain development, and neuron recognition.

The genes in the black module were significantly enriched for neuroactive ligand–receptor interaction, systemic lupus erythematosus, and CAMP signaling pathway. Carbohydrate

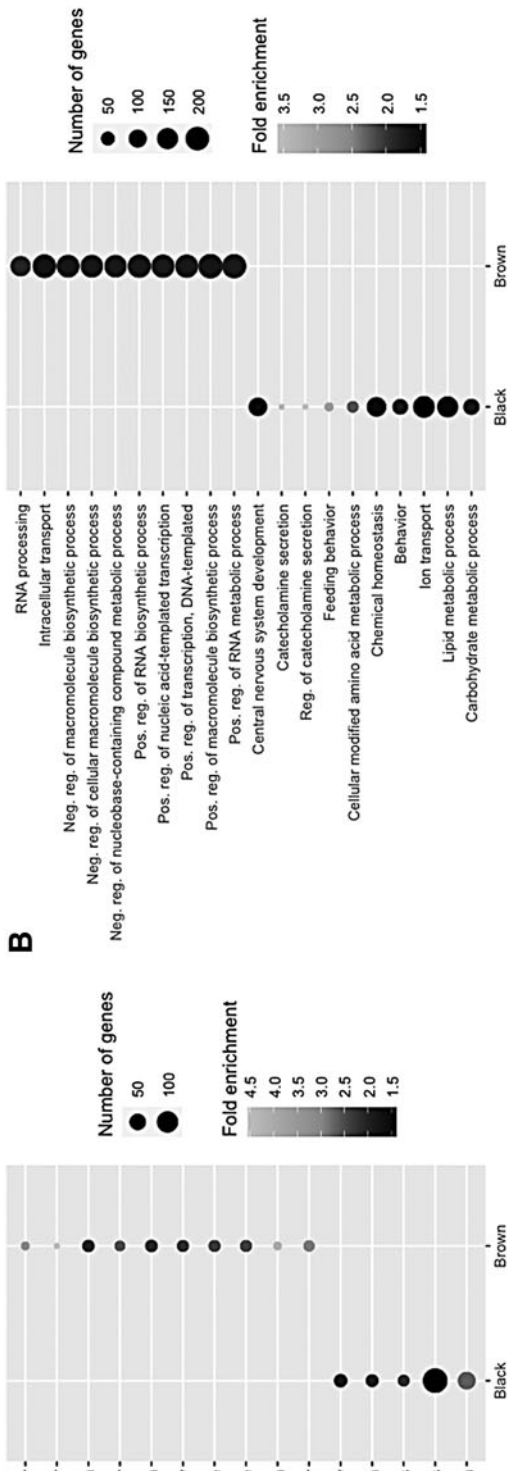

FIG. 3. Functional enrichment analysis of key module genes. **(A)** Top-10 significantly enriched KEGG pathways of module genes **(B)** Top-10 significantly enriched GO BP terms of module genes. BP, biological process; GO, Gene Ontology; KEGG, Kyoto Encyclopedia of Genes and Genomes.

and lipid metabolism, catecholamine secretion, nervous system development, forebrain development, and synaptic signaling were found among the significantly enriched BPs in this module.

Identification and validation of hub genes

The hub genes of key modules were explored based on GS and MM values to better represent the clinical signatures, and a total of 1550 genes ($|MM| > 0.8$ and $|GS| > 0.5$) were identified as WGCNA hubs. Furthermore, PPI networks were reconstructed around the genes in key modules, and the modular analyses of the black PPI network consisted of 1367 interactions between 643 proteins, and the brown PPI network consisted of 3146 interactions between 895 proteins, revealed a total of 205 PPI hubs (63 and 142 hubs in the black and brown PPI networks, respectively). The intersection of WGCNA hubs, PPI hubs, and DEGs of the GSE15197 dataset were then selected as core genes. The 38 commonly identified core genes were further analyzed.

Two independent gene expression datasets, GSE113439 and GSE53408, were used to validate the core genes as candidate biomarkers for IPAH. Among these genes, *DDX52*, *ESF1*, *HNRNPA3*, *MYO5A*, *RFC1*, and *RSRC1* were also found to be differentially expressed in both GSE113439 and GSE53408 datasets (Supplementary Table S1), and were therefore considered as key gene signatures in IPAH.

Key genes included DEAD-box helicase 52 (*DDX52*), nucleolar pre-rRNA processing protein (*ESF1*), and heterogeneous nuclear ribonucleoprotein A3 (*HNRNPA3*), which enable RNA binding activity. Myosin VA (*MYO5A*), which is a member of the myosin gene superfamily, has functions in melanosome transport, and mediates the transport of vesicles to the plasma membrane. Replication factor C subunit 1 (*RFC1*) encodes the large subunit of replication factor C, and acts as an activator of DNA polymerases, binding to the 3′ end of primers, and promoting coordinated synthesis of both strands. Arginine and serine-rich coiled-coil 1 (*RSRC1*) encodes a member of the serine and arginine-rich–related protein family. The encoded protein plays a role in both constitutive and alternative pre-mRNA splicing and transcriptional regulation.

The diagnostic abilities of the key genes were examined using ROC curves (Fig. 4). The AUC values for *DDX52*, *ESF1*, *HNRNPA3*, *MYO5A*, *RFC1*, and *RSRC1* indicated their significantly high performance (AUC value ≥70%) in discriminating IPAH patients from healthy controls, and therefore these genes were accepted as diagnostic and considered as drug targets.

Potential drugs identified by drug repositioning

A drug repurposing methodology was applied using CMAP data to predict drugs targeting the proteins encoded by *DDX52*, *ESF1*, *HNRNPA3*, *MYO5A*, *RFC1*, and *RSRC1*. Because these genes were upregulated in the presence of IPAH, drugs that downregulate their expression were investigated. After eliminating duplicated and unknown drugs, a total of 13 potential drugs with q-value <0.05 were found to downregulate *DDX52*, *ESF1*, *HNRNPA3*, *MYO5A*, and *RFC1* (Table 1). No drug candidates were identified that downregulated *RSRC1*.

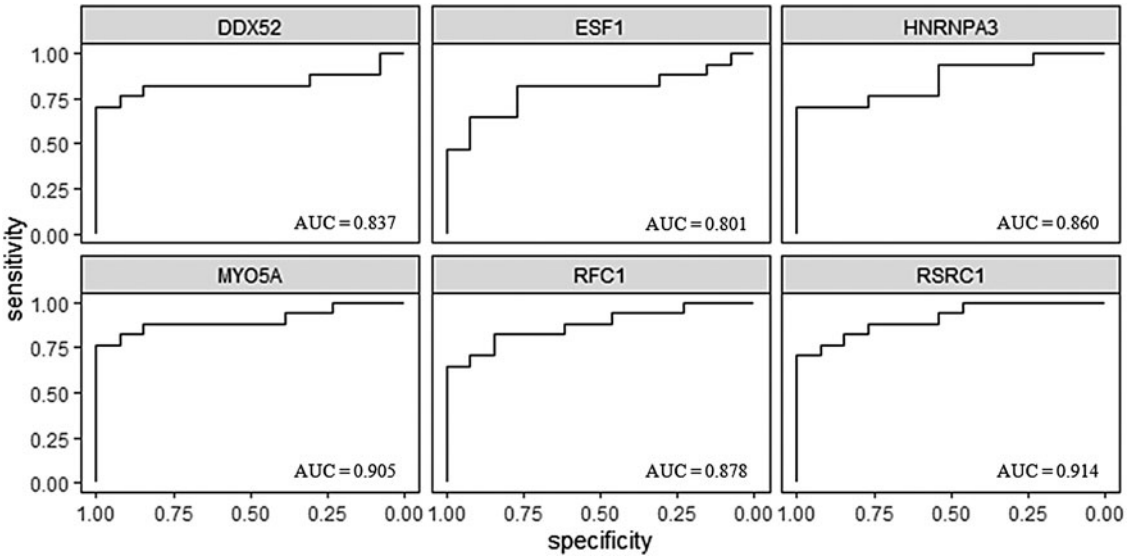

FIG. 4. ROC curves of the key genes. ROC, receiver operating characteristic.

Discussion

IPAH is a rare but serious disease associated with significant morbidity and mortality. The pathogenesis of the disease still remains unclear. Moreover, the lack of robust molecular signatures is a barrier to therapeutic target and diagnostic discovery and development (Boucherat et al., 2017).

In this study, integrative multi-omics analyses of genome-wide expression data were performed to elucidate the underlying mechanisms of IPAH pathogenesis. The molecular profiling of IPAH was evaluated at the gene and miRNA expression levels by identifying DEGs, DEmiRNAs, and the associated molecular mechanisms. Evaluation of regulatory associations between DEGs and DEmiRNAs identified miRNAs that could be further developed as potential prognostic biomarkers.

In addition, a weighted gene coexpression network was constructed and linked to the human PPI network to identify key genes of IPAH using a network-based methodology. Modularity analysis of the constructed networks revealed the presence of common hub proteins, which were used to perform a comprehensive drug repositioning analysis. Several drugs including senolytics, alkaloids, cardiac glycosides, insulin sensitizers, and drugs with antifibrotic, anti-inflammatory, and antiproliferative effects, were suggested as potential drug candidates for IPAH.

Individual analysis of the gene expression dataset GSE15197 revealed numerous, thousands, of DEGs. However, to uncover the mechanisms behind IPAH, I combined information from gene and miRNA expression datasets, and evaluated the disease by elucidating the regulatory associations between the identified DEGs and DEmiRNAs. Overrepresentation analyses revealed significant molecular pathways and BPs. Several cancer and cancer-related pathways were found to be significantly upregulated. PAH has previously been reported to share common pathological features with cancer (Zeng et al., 2021). PAH and cancer cells show similarities in their exposure to stressful conditions, and the acquired stress tolerance of the cells allows them to survive and proliferate over time (Boucherat et al., 2017).

In addition to excessive proliferation, immune cell infiltration is a common feature of cancer and PAH (Cool et al., 2020). As expected, pathways and processes related to cardiovascular disease (CVD), lipid metabolism, and the endocrine system were also found to be significantly associated with IPAH. Lipid metabolism, particularly oxidized lipids, has been shown to contribute to many pathways involved in the pathogenesis of PAH, including vascular remodeling, mitochondrial dysfunction, proliferation and resistance to apoptosis, vasoconstriction, and endothelial dysfunction (Sharma et al., 2016). Insulin resistance in PAH patients has also been characterized by alterations in lipid metabolism and the high-density lipoprotein cholesterol fraction (Hemnes et al., 2019; Jonas and Kopeć, 2019).

Table 1. Potential Drug Candidates Targeting the Key Genes Associated with Pulmonary Arterial Hypertension

Targets	*Potential drugs/compounds*
DDX52	Cephaeline, digoxigenin, helveticoside, lanatoside C, LY294002, phenoxybenzamine, trichostatin A
ESF1	Cephaeline, genistein, pioglitazone, rosiglitazone, trichostatin A
HNRNPA3	Lanatoside C
MYO5A	LY294002, tanespimycin
RFC1	Trichostatin A, tanespimycin, geldanamycin, LY294002, alvespimycin

DDX52, DEAD-box helicase 52; *HNRNPA3*, heterogeneous nuclear ribonucleoprotein A3; *RFC1*, replication factor C subunit 1.

The gene coexpression network reconstructed using GSE15197 IPAH data revealed two key modules via WGCNA and module–trait relationship analyses. To increase the reliability and robustness of the results, a combined intramodular connectivity was considered in the WGCNA key modules and PPI networks reconstructed around the proteins encoded by module genes. A total of 38 genes were identified as common hubs, and cross-validation analysis, followed by diagnostic performance analysis that established six key genes (*DDX52*, *ESF1*, *HNRNPA3*, *MYO5A*, *RFC1*, and *RSRC1*) as the final candidate gene signatures.

MYO5A, which is one of the three myosin V heavy-chain genes, has previously been shown to be associated with PAH. Smooth muscle myosin has been implicated in vasoconstriction in PAH, and a smooth muscle myosin inhibitor has been reported to relax pulmonary artery vascular rings in both acute and chronic rat models of PAH (Ho et al., 2012). Although not previously associated with PAH, *DDX52*, *ESF1*, *HNRNPA3*, *RFC1*, and *RSRC1* are involved in a various CVDs, vascular remodeling, and proliferation.

Bioinformatic analysis identified *DDX52* as a characteristic gene in heart failure (Li et al., 2022). In addition, two members of the DEAD-box family of RNA helicases, *DDX46* and *DDX5*, have been reported to be associated with PAH and vascular remodeling, respectively. *DDX46* was found to be significantly upregulated in chickens with PAH (Li et al., 2021a), and *DDX5* exerted a protective effect against smooth muscle cell proliferation and vascular remodeling (Fan et al., 2019). A meta-analysis of PAH-associated transcriptomic data revealed *ESF1* as commonly upregulated (Li et al., 2020). Although the role of *HNRNPA3* remains unclear, increased activity of protein arginine methyltransferases, which catalyze arginine methylation of most of the heterogeneous nuclear ribonucleoproteins, has been linked to several CVDs (Couto e Silva et al., 2020; Wu et al., 2021).

RFC1 is a subunit of the replication factor C family, which may play a pivotal role in cancer cell proliferation, progression, invasion, and metastasis (Li et al., 2018). *RSRC1* interacts with the transcription factor *ERB2*, which plays an important role in CVD (Perez et al., 2018). To the best of my knowledge, this study is the first to propose the association of *DDX52*, *ESF1*, *HNRNPA3*, *RFC1*, and *RSRC1* with PAH.

Dysregulation of miRNAs contributes to the development and severity of PAH, and therefore miRNA targets play an important role in developing therapeutic strategies to reverse vascular remodeling and proliferation (Carregal-Romero et al., 2020; Grant et al., 2013). From a holistic perspective, a number of active regulatory mechanisms were identified, and represented by interactions between key genes and DEmiRNAs (Supplementary Fig. S3). Considering these associations, seven DEmiRNAs, including miR-495-5p, miR-500a-3p, miR-198, miR-517a-3p, miR-302f, miR-375 and miR-31-5p, were prominent.

Inhibition of miR-495 was reported to improve hemodynamics, vascular remodeling, and angiogenesis in PAH model (Fu et al., 2019). Although miR-500a-3p was not found to be associated with PAH, it was shown to be involved in several types of cancer (Esposti et al., 2017; Jiang et al., 2017; Long et al., 2022). miR-198 was found to play a role in neural development, cell cycle regulation, proliferation, invasion, migration, apoptosis and drug resistance, and alterations in its expression were associated with various cancers (Kaushik and Kumar, 2022; Wang et al., 2022). miR-517a-3p contributed to cell proliferation, migration, and invasion in lung cancer (Jin et al., 2014). The miR-302 family was reported to be involved in cardiomyocyte function, heart development, and regeneration in mice (Tian et al., 2015), and was also found to induce regeneration in lung tissue of *Streptococcus pneumoniae*–infected mice (Wang et al., 2019a).

Altered expression of miR-375 was observed in three subtypes of lung cancer, including adenocarcinoma, small cell lung carcinoma, and squamous cell carcinoma (Jin et al., 2015). In addition, miR-375 was identified as a smoking-induced miRNA in patients with chronic obstructive pulmonary disease (van Nijnatten et al., 2022). miR-375-3p was upregulated in maternal serum of women with fetal congenital heart disease (Li et al., 2021b). miR-31-5p promotes cell migration in several cancers. In addition, increased expression of miR-31-5p was found to contribute to oxidative stress and vascular smooth muscle cell migration in spontaneously hypertensive rats (Zhou et al., 2021).

These associations suggest that the resulting regulatory interactions may represent the changes in both vascular remodeling and proliferation during PAH pathogenesis and therefore, the identified miRNAs may be evaluated as potential markers for screening and therapeutic purposes in PAH.

Key gene-based drug repositioning identified alvespimycin, tanespimycin, geldanamycin, LY294002, cephaeline, digoxigenin, lanatoside C, helveticoside, trichostatin A, phenoxybenzamine, genistein, pioglitazone, and rosiglitazone as drugs with the potential to reverse gene expression (Supplementary Table S2).

Alvespimycin, tanespimycin, and geldanamycin are HSP90 inhibitors. Tanespimycin treatment has been shown to prevent the progression of PAH in a rat model, possibly by reducing inflammation through HSP90 inhibition (Wang et al., 2016). HSP90 inhibitors have senolytic activity, and senolytic drugs may hold promise for the treatment of age-related diseases or conditions associated with the burden of senescent cells (Fuhrmann-Stroissnigg et al., 2017). Mitochondrial HSP90 accumulation has been reported to contribute to vascular remodeling in PAH, and *in vivo* experiments showed that gamitrinib, a mitochondria-targeted HSP90 inhibitor, ameliorated PAH by reversing pulmonary vascular remodeling in two rat models (Boucherat et al., 2018).

LY294002 was a common drug found for *DDX52*, *MYO5A*, and *RFC1*. It acts as an mTOR, PI3K, DNA-dependent protein kinase, phosphodiesterase, and PLK inhibitor. Inhibition of PI3K/Akt signaling by LY294002 in a rat model of PAH resulted in suppression of medial smooth muscle cell proliferation but had no effect on pulmonary artery pressure, possibly because of dose (Garat et al., 2013). LY294002 was shown to reduce proliferation and chemotaxis of human pulmonary arterial smooth muscle cells in a concentration-dependent manner (Berghausen et al., 2021).

Cephaeline, the major alkaloid of ipecac, modulates G-quadruplex (G4)-dependent alternative splicing (Zhang et al., 2019). G4 formation plays a role in vital cellular functions such as transcription, translation, telomere elongation, and maintenance of genome stability. G4 structures have been proposed as promising therapeutic targets in several cancers (Varshney et al., 2020). In addition, emetine, an analog of cephaeline, was found to inhibit pulmonary artery smooth muscle cell proliferation, and ameliorate PAH in rat models (Siddique et al., 2019).

Digoxigenin, lanatoside C, and helveticoside are cardiac glycosides. Cardiac glycosides increase the force of cardiac contractions by binding to estrogen receptors or inhibiting Na^+/K^+ ATPase (Chao et al., 2017; Kim et al., 2015). Lanatoside C has been demonstrated to induce apoptosis of human glioblastoma and hepatocellular carcinoma cells (Badr et al., 2011; Chao et al., 2017). Helveticoside has been shown to be cytotoxic to human cancer cell lines (Kim et al., 2015; Lee et al., 2013). Given their ability to increase cardiac output, and inhibit malignant cell proliferation, the identified cardiac glycosides may have a potential role as therapeutic agents against PAH.

Trichostatin A, a histone deacetylase (HDCA) inhibitor, was a common drug found for *DDX52*, *ESF1*, and *RFC1*. Given the contribution of HDCA activity to vascular remodeling in PAH, Zhao et al. investigated the efficacy of two HDCA inhibitors, valproic acid, and suberoylanilide hydroxamic acid, and found that they reverse total histone levels in PAH models (Zhao et al., 2012). Trichostatin A was found to have antifibrotic and anti-inflammatory effects in adult mouse cardiac fibroblasts, supporting a potential role as a therapeutic agent to reverse remodeling in inflammatory heart disease (Somanna et al., 2016).

Phenoxybenzamine, an adrenergic receptor antagonist, is used to treat pheochromocytoma and episodes of hypertension and sweating. It has also been shown to have antiproliferative effects on human tumor cell cultures (Inchiosa, 2018). One of the tyrosine kinase inhibitors, genistein, is a natural phytoestrogen derived from soy. The protective effect of estrogen against CVD has already been demonstrated (Iorga et al., 2017; Murphy, 2011). Genistein therapy was shown to attenuate PAH and reverse cardiopulmonary function and structure abnormalities in rats (Matori et al., 2012). In addition, genistein inhibited hypertrophy of hypoxia-treated pulmonary artery smooth muscle cells isolated from chick embryos (Zhang et al., 2018b).

Pioglitazone and rosiglitazone are insulin sensitizers and PPAR receptor agonists. In a rat model of PAH, oral pioglitazone has been demonstrated to prevent right ventricular heart failure and ameliorate PAH by modulating miRNAs involved in fatty acid metabolism (Legchenko et al., 2018). Rosiglitazone treatment has also been shown to reduce pulmonary hypertension in chronically hypoxic rats (Kim et al., 2010). Considering the potential association between insulin resistance and PAH (Hansmann et al., 2007), these two insulin-sensitizing agents warrant further consideration in future clinical drug development and IPAH translational research.

This study identified a total of 13 candidate drugs including senolytics, alkaloids, cardiac glycosides, insulin sensitizers, and drugs with antifibrotic, anti-inflammatory, and antiproliferative effects, for consideration in future clinical drug development. Despite the significant results obtained here, further *in vitro* and *in vivo* studies should be conducted to evaluate the performance of the proposed repositioned drugs.

Conclusions

IPAH is a progressive and debilitating disease that affects the pulmonary arteries, resulting in increased pulmonary vascular resistance and right ventricular dysfunction, and associated with marked morbidity and mortality (Schlueter et al., 2020; Swaminathan et al., 2020). Elucidating the molecular mechanisms underlying IPAH pathogenesis is essential for developing novel systems biomarkers, diagnostics, and therapeutics. In this study, comparative analysis of mRNA and miRNA expression data revealed active regulatory associations in disease pathogenesis, and deciphered disease-specific gene and miRNA signatures. The study identified *DDX52*, *ESF1*, *HNRNPA3*, *MYO5A*, *RFC1*, and *RSRC1* as key gene signatures associated with IPAH. The transcriptional reprogramming of these genes was found to be regulated by seven DEmiRNAs (miR-495-5p, miR-500a-3p, miR-198, miR-517a-3p, miR-302f, miR-375, and miR-31-5p), which are noteworthy as potential novel biomarker candidates.

In addition, key gene-based drug repositioning analysis identified alvespimycin, tanespimycin, geldanamycin, LY294002, cephaeline, digoxigenin, lanatoside C, helveticoside, trichostatin A, phenoxybenzamine, genistein, pioglitazone, and rosiglitazone as potential drug candidates for future clinical drug development for IPAH. Although this study provides molecular signatures and signature-based repositioned drug candidates through multi-omics data integration, future studies are needed to evaluate their clinical value as diagnostics and therapeutics for IPAH.

Authors' Contributions

C.K. conceived the study, carried out the analyses, interpreted the results, and wrote the article.

Author Disclosure Statement

The author declares there are no conflicting financial interests.

Funding Information

This research did not receive any specific grant from funding agencies in the public, commercial, or not-for-profit sectors.

Supplementary Material

Supplementary Figure S1
Supplementary Figure S2
Supplementary Figure S3
Supplementary Table S1
Supplementary Table S2

References

Ashburner M, Ball CA, Blake JA, et al. Gene Ontology: Tool for the unification of biology. The Gene Ontology Consortium. Nat Genet 2000;25(1):25–29; doi: 10.1038/75556

Auwul R, Rahman R, Gov E, et al. Bioinformatics and machine learning approach identifies potential drug targets and pathways in Covid-19. Brief Bioinform 2021;22(5):bbab120; doi: 10.1093/bib/bbab120

Bader GD, Hogue CWV. An automated method for finding molecular complexes in large protein interaction networks. BMC Bioinformatics 2003;4:2; doi: 10.1186/1471-21065-4-2.

Badr CE, Wurdinger T, Nilsson J, et al. Lanatoside C sensitizes glioblastoma cells to tumor necrosis factor-related apoptosi-

sinducing ligand and induces an alternative cell death pathway. Neuro Oncol 2011;13(11):1213–1224; doi: 10.1093/neuonc/nor067

Barrett T, Edgar R. Mining microarray data at NCBI's Gene Expression Omnibus (GEO). Methods Mol Biol 2006;338:175–190; doi: 10.1385/1-59745-097-9:175

Berghausen EM, Janssen W, Vantler M, et al. Disrupted PI3K subunit P110α signaling protects against pulmonary hypertension and reverses established disease in rodents. J Clin Invest 2021;131(19):e136939; doi: 10.1172/JCI136939

Boucherat O, Peterlini T, Bourgeois A, et al. Mitochondrial HSP90 accumulation promotes vascular remodeling in pulmonary arterial hypertension. Am J Respir Crit Care Med 2018;198(1):90–103; doi: 10.1164/rccm.201708-1751OC

Boucherat O, Vitry G, Trinh I, et al. The cancer theory of pulmonary arterial hypertension. Pulm Circ 2017;7(2):285–299; doi: 10.1177/2045893217701438

Brohawn DG, O'Brien LC, Bennett Jr JP. RNAseq analyses identify tumor necrosis factor-mediated inflammation as a major abnormality in ALS spinal cord. PLoS One 2016;11(8):e0160520; doi: 10.1371/journal.pone.0160520

Carregal-Romero S, Fadón L, Berra E, et al. MicroRNA nanotherapeutics for lung targeting. Insights into pulmonary hypertension. Int J Mol Sci 2020;21(9):3253; doi: 10.3390/ijms21093253

Chao MW, Chen TH, Huang HL, et al. Lanatoside C, a cardiac glycoside, acts through protein kinase Cδ to cause apoptosis of human hepatocellular carcinoma cells. Sci Rep 2017;7:46134; doi: 10.1038/srep46134

Cool CD, Kuebler WM, Bogaard HJ, et al. The hallmarks of severe pulmonary arterial hypertension: The cancer hypothesis-ten years later. Am J Physiol Lung Cell Mol Physiol 2020;318(6):L1115–L1130; doi: 10.1152/ajplung.00476.2019

Couto e Silva A, Wu CYC, Citadin CT, et al. Protein arginine methyltransferases in cardiovascular and neuronal function. Mol Neurobiol 2020;57(3):1716–1732; doi: 10.1007/s12035-019-01850-z

Esposti DD, Aushev VN, Lee E, et al. MiR-500a-5p regulates oxidative stress response genes in breast cancer and predicts cancer survival. Sci Rep 2017;7(1):15966; doi: 10.1038/s41598-017-16226-3

Fan Y, Chen Y, Zhang J, et al. Protective role of RNA helicase dead-box protein 5 in smooth muscle cell proliferation and vascular remodeling. Circ Res 2019;124(10):E84–E100; doi: 10.1161/CIRCRESAHA.119.314062

Fu J, Bai P, Chen Y, et al. Inhibition of miR-495 improves both vascular remodeling and angiogenesis in pulmonary hypertension. J Vasc Res 2019;56(2):97–106; doi: 10.1159/000500024

Fuhrmann-Stroissnigg H, Ling YY, Zhao J, et al. Identification of HSP90 inhibitors as a novel class of senolytics. Nat Commun 2017;8(1):422; doi: 10.1038/s41467-017-00314-z

Galiè N, Humbert M, Vachiery JL, et al. 2015 ESC/ERS guidelines for the diagnosis and treatment of pulmonary hypertension. Eur Respir J 2015;46(4):903–975; doi: 10.1183/13993003.01032-2015

Garat CV, Crossno JT, Sullivan TM, et al. Inhibition of phosphatidylinositol 3-kinase/Akt signaling attenuates hypoxia-induced pulmonary artery remodeling and suppresses CREB depletion in arterial smooth muscle cells. J Cardiovasc Pharmacol 2013;62(6):539–548; doi: 10.1097/FJC.0000000000000014

Grant JS, White K, MacLean MR, et al. MicroRNAs in pulmonary arterial remodeling. Cell Mol Life Sci 2013;70(23):4479–4494; doi: 10.1007/s00018-013-1382-5

Hansmann G, Wagner RA, Schellong S, et al. Pulmonary arterial hypertension is linked to insulin resistance and reversed by peroxisome proliferator-activated receptor-γ activation. Circulation 2007;115(10):1275–1284; doi: 10.1161/CIRCULATIONAHA.106.663120

Hemnes AR, Luther JM, Rhodes CJ, et al. Human PAH is characterized by a pattern of lipid-related insulin resistance. JCI Insight 2019;4(1):e123611; doi: 10.1172/jci.insight.123611

Hendriks PM, Staal DP, van de Groep LD, et al. The evolution of survival of pulmonary arterial hypertension over 15 years. Pulm Circ 2022;12(4):e12137; doi: 10.1002/pul2.12137

Ho D, Chen L, Zhao X, et al. Smooth muscle myosin inhibition: A novel therapeutic approach for pulmonary hypertension. PLoS One 2012;7(5):e36302; doi: 10.1371/journal.pone.0036302

Huang HY, Lin YCD, Cui S, et al. MiRTarBase update 2022: An informative resource for experimentally validated miRNA-target interactions. Nucleic Acids Res 2022;50(D1):D222–D230; doi: 10.1093/nar/gkab1079

Inchiosa MA. Anti-tumor activity of phenoxybenzamine and its inhibition of histone deacetylases. PLoS One 2018;13(6):e0198514; doi: 10.1371/journal.pone.0198514

Iorga A, Cunningham CM, Moazeni S, et al. The protective role of estrogen and estrogen receptors in cardiovascular disease and the controversial use of estrogen therapy. Biol Sex Differ 2017;8(1):33; doi: 10.1186/s13293-017-0152-8

Jiang C, Long J, Liu B, et al. MiR-500a-3p promotes cancer stem cells properties via STAT3 pathway in human hepatocellular carcinoma. J Exp Clin Cancer Res 2017;36(1):99; doi: 10.1186/s13046-017-0568-3

Jin J, Zhou S, Li C, et al. MiR-517a-3p accelerates lung cancer cell proliferation and invasion through inhibiting FOXJ3 expression. Life Sci 2014;108(1):48–53; doi: 10.1016/j.lfs.2014.05.006

Jin Y, Liu Y, Zhang J, et al. The expression of MIR-375 is associated with carcinogenesis in three subtypes of lung cancer. PLoS One 2015;10(12):e0144187; doi: 10.1371/journal.pone.0144187

Jonas K, Kopeć G. HDL cholesterol as a marker of disease severity and prognosis in patients with pulmonary arterial hypertension. Int J Mol Sci 2019;20(14):3514; doi: 10.3390/ijms20143514

Kamburov A, Stelzl U, Lehrach H, et al. The ConsensusPathDB interaction database: 2013 update. Nucleic Acids Res 2013;41(Database Issue):D793–D800; doi: 10.1093/nar/gks1055

Kanehisa M, Goto S. KEGG: Kyoto Encyclopedia of Genes and Genomes. Nucleic Acids Res 2000;28(1):27–30; doi: 10.1093/nar/28.1.27

Kaushik P, Kumar A. Emerging role and function of MiR-198 in human health and diseases. Pathol Res Pract 2022;229:153741; doi: 10.1016/j.prp.2021.153741

Kim BY, Lee J, Kim NS. Helveticoside is a biologically active component of the seed extract of descurainia sophia and induces reciprocal gene regulation in A549 human lung cancer cells. BMC Genomics 2015;16(1):713; doi: 10.1186/s12864-015-1918-1

Kim EK, Lee JH, Oh YM, et al. Rosiglitazone attenuates hypoxia-induced pulmonary arterial hypertension in rats. Respirology 2010;15(4):659–668; doi: 10.1111/j.1440-1843.2010.01756.x

Lamb J, Crawford ED, Peck D, et al. The connectivity map: Using gene-expression signatures to connect small molecules,

genes, and disease. Science 2006;313(5795):1929–1935; doi: 10.1126/science.1132939

Langfelder P, Horvath S. WGCNA: An R package for weighted correlation network analysis. BMC Bioinformatics 2008;9: 559; doi: 10.1186/1471-2105-9-559

Lee YJ, Kim NS, Kim H, et al. Cytotoxic and anti-inflammatory constituents from the seeds of descurainia sophia. Arch Pharm Res 2013;36(5):536–541; doi: 10.1007/s12272-013-0066-x

Legchenko E, Chouvarine P, Borchert P, et al. PPARγ agonist pioglitazone reverses pulmonary hypertension and prevents right heart failure via fatty acid oxidation. Sci Transl Med 2018;10(438):eaao0303; doi: 10.1126/scitranslmed.aao0303

Li A, He J, Zhang Z, et al. Integrated bioinformatics analysis reveals marker genes and potential therapeutic targets for pulmonary arterial hypertension. Genes (Basel) 2021a;12(9): 1339; doi: 10.3390/genes12091339

Li J, Zhang X, Ren P, et al. Landscape of RNA-binding proteins in diagnostic utility, immune cell infiltration and PANoptosis features of heart failure. Front Genet 2022;13:1004163; doi: 10.3389/fgene.2022.1004163

Li Q, Meng LB, Liu DP. Screening and identification of therapeutic targets for pulmonary arterial hypertension through microarray technology. Front Genet 2020;11:782; doi: 10.3389/fgene.2020.00782

Li Y, Gan S, Ren L, et al. Multifaceted regulation and functions of replication factor C family in human cancers. Am J Cancer Res 2018;8(8):1343–1355.

Li Y, Li X, Wang L, et al. MiR-375-3p contributes to hypoxia-induced apoptosis by targeting Forkhead Box P1 (FOXP1) and Bcl2 like Protein 2 (Bcl2l2) in rat cardiomyocyte H9c2 cells. Biotechnol Lett 2021b;43(2):353–367; doi: 10.1007/s10529-020-03013-w

Long J, Liu B, Yao Z, et al. MiR-500a-3p is a potential prognostic biomarker in hepatocellular carcinoma. Int J Gen Med 2022;15:1891–1899; doi: 10.2147/IJGM.S340629

Luo J, Li H, Liu Z, et al. Integrative analyses of gene expression profile reveal potential crucial roles of mitotic cell cycle and microtubule cytoskeleton in pulmonary artery hypertension. BMC Med Genomics 2020;13(1):86; doi: 10.1186/s12920-020-00740-x

Matori H, Umar S, Nadadur RD, et al. Genistein, a soy phytoestrogen, reverses severe pulmonary hypertension and prevents right heart failure in rats. Hypertension 2012;60(2): 425–430; doi: 10.1161/HYPERTENSIONAHA.112.191445

Mayeux JD, Pan IZ, Dechand J, et al. Management of pulmonary arterial hypertension. Curr Cardiovasc Risk Rep 2021; 15(1):2; doi: 10.1007/s12170-020-00663-3

Mura M, Cecchini MJ, Joseph M, et al. Osteopontin lung gene expression is a marker of disease severity in pulmonary arterial hypertension. Respirology 2019;24(11):1104–1110; doi: 10.1111/resp.13557

Murphy E. Estrogen signaling and cardiovascular disease. Circ Res 2011;109(6):687–696; doi: 10.1161/CIRCRESAHA.110.236687

van Nijnatten J, Brandsma CA, Steiling K, et al. High MiR203a-3p and MiR-375 expression in the airways of smokers with and without COPD. Sci Rep 2022;12(1):5610; doi: 10.1038/s41598-022-09093-0

Perez Y, Menascu S, Cohen I, et al. RSRC1 mutation affects intellect and behaviour through aberrant splicing and transcription, downregulating IGFBP3. Brain 2018;141(4):961–970; doi: 10.1093/brain/awy045

R Core Team. R: A Language and Environment for Statistical Computing. R Foundation for Statistical Computing: Vienna, Austria; 2020. Available from: www.r-project.org/index.html

Rajkumar R, Konishi K, Richards TJ, et al. Genomewide RNA expression profiling in lung identifies distinct signatures in idiopathic pulmonary arterial hypertension and secondary pulmonary hypertension. Am J Physiol Heart Circ Physiol 2010;298(4):H1235–H1248; doi: 10.1152/ajpheart.00254.2009

Schlueter M, Beaudet A, Davies E, et al. Evidence synthesis in pulmonary arterial hypertension: A systematic review and critical appraisal. BMC Pulm Med 2020;20(1):202; doi: 10.1186/s12890-020-01241-4

Shannon P, Markiel A, Ozier O, et al. Cytoscape: A software environment for integrated models of biomolecular interaction networks. Genome Res 2003;13(11):2498–2504; doi: 10.1101/gr.1239303

Sharma S, Ruffenach G, Umar S, et al. Role of oxidized lipids in pulmonary arterial hypertension. Pulm Circ 2016;6(3): 261–273; doi: 10.1086/687293

Siddique MAH, Satoh K, Kurosawa R, et al. Identification of emetine as a therapeutic agent for pulmonary arterial hypertension: Novel effects of an old drug. Arterioscler Thromb Vasc Biol 2019;39(11):2367–2385; doi: 10.1161/ATVBAHA.119.313309

Smyth GK. Linear models and empirical bayes methods for assessing diferential expression in microarray experiments. Stat Appl Genet Mol Biol 2004;3:Article3; doi: 10.2202/1544-6115.1027

Somanna NK, Valente AJ, Krenz M, et al. Histone deacetyltransferase inhibitors trichostatin A and mocetinostat differentially regulate MMP9, IL-18 and RECK expression, and attenuate angiotensin II-induced cardiac fibroblast migration and proliferation. Hypertens Res 2016;39(10):709–716; doi: 10.1038/hr.2016.54

Swaminathan AC, Zhu H, Tapson V, et al. Treatment-related biomarkers in pulmonary hypertension patients on oral therapies. Respir Res 2020;21(1):304; doi: 10.1186/s12931-020-01566-y

Szklarczyk D, Gable AL, Nastou KC, et al. The STRING Database in 2021: Customizable protein-protein networks, and functional characterization of user-uploaded gene/measurement sets. Nucleic Acids Res 2021;49(D1):D605–D612; doi: 10.1093/nar/gkaa1074

Tian Y, Liu Y, Wang T, et al. A MicroRNA-hippo pathway that promotes cardiomyocyte proliferation and cardiac regeneration in mice. Sci Transl Med 2015;7(279):279ra38; doi: 10.1126/scitranslmed.3010841

Varshney D, Spiegel J, Zyner K, et al. The regulation and functions of DNA and RNA G-Quadruplexes. Nat Rev Mol Cell Biol 2020;21(8):459–474; doi: 10.1038/s41580-020-0236-x

Wang GK, Li SH, Zhao ZM, et al. Inhibition of heat shock protein 90 improves pulmonary arteriole remodeling in pulmonary arterial hypertension. Oncotarget 2016;7(34):54263–54273; doi: 10.18632/oncotarget.10855

Wang X, Zhu Y, Xie Q. The promising role and prognostic value of MiR-198 in human diseases. Am J Transl Res 2022;14(4):2749–2766.

Wang Y, Li Y, Zhang P, et al. Regenerative therapy based on MiRNA-302 mimics for enhancing host recovery from pneumonia caused by Streptococcus Pneumoniae. PNAS 2019a;116(17):8493–8498; doi: 10.1073/pnas.1818522116

Wang Z, He E, Sani K, et al. Drug Gene Budger (DGB): An application for ranking drugs to modulate a specific gene

based on transcriptomic signatures. Bioinformatics 2019b; 35(7):1247–1248; doi: 10.1093/bioinformatics/bty763

Wang Z, Lachmann A, Keenan AB, et al. L1000FWD: Fireworks visualization of drug-induced transcriptomic signatures. Bioinformatics 2018;34(12):2150–2152; doi: 10.1093/bioinformatics/bty060

Wishart DS, Feunang YD, Guo AC, et al. DrugBank 5.0: A major update to the drugbank database for 2018. Nucleic Acids Res 2018;46(D1):D1074–D1082; doi: 10.1093/nar/gkx1037

Wu D, Talbot CC, Liu Q, et al. Identifying MicroRNAs targeting Wnt/β-catenin pathway in end-stage idiopathic pulmonary arterial hypertension. J Mol Med (Berl) 2016; 94(8):875–885; doi:10.1007/s00109-016-1426-z

Wu Q, Schapira M, Arrowsmith CH, et al. Protein arginine methylation: from enigmatic functions to therapeutic targeting. Nat Rev Drug Discov 2021;20(7):509–530; doi: 10.1038/s41573-021-00159-8

Yan S. Integrative analysis of promising molecular biomarkers and pathways for coronary artery disease using WGCNA and MetaDE methods. Mol Med Rep 2018;18(3):2789–2797; doi: 10.3892/mmr.2018.9277

Zeng Y, Li N, Zheng Z, et al. Screening of key biomarkers and immune infiltration in pulmonary arterial hypertension via integrated bioinformatics analysis. Bioengineered 2021; 12(1):2576–2591; doi: 10.1080/21655979.2021.1936816

Zhang Q, Ma C, Gearing M, et al. Integrated proteomics and network analysis identifies protein hubs and network alterations in Alzheimer's disease. Acta Neuropathol Commun 2018a;6(1):19; doi: 10.1186/s40478-018-0524-2

Zhang J, Harvey SE, Cheng C. A high-throughput screen identifies small molecule modulators of alternative splicing by targeting RNA G-quadruplexes. Nucleic Acids Res 2019; 47(7):3667–3679; doi: 10.1093/nar/gkz036

Zhang M, Wu Y, Wang M, et al. Genistein rescues hypoxia-induced pulmonary arterial hypertension through estrogen receptor and β-adrenoceptor signaling. J Nutr Biochem 2018b;58:110–118; doi: 10.1016/j.jnutbio.2018.04.016

Zhao L, Chen CN, Hajji N, et al. Histone deacetylation inhibition in pulmonary hypertension: Therapeutic potential of valproic acid and suberoylanilide hydroxamic acid. Circulation 2012;126(4):455–467; doi: 10.1161/CIRCULATIONAHA.112.103176

Zhao YD, Yun HZH, Peng J, et al. De novo synthesize of bile acids in pulmonary arterial hypertension lung. Metabolomics 2014;10(6):1169–1175; doi: 10.1007/s11306-014-0653-y

Zhou B, Wu LL, Zheng F, et al. Mir-31-5p promotes oxidative stress and vascular smooth muscle cell migration in spontaneously hypertensive rats via inhibiting Fndc5 expression. Biomedicines 2021;9(8):1009; doi: 10.3390/biomedicines9081009

Address correspondence to:
Ceyda Kasavi, PhD
Department of Bioengineering
Faculty of Engineering
Marmara University
Istanbul 34722
Turkey

E-mail: ceyda.kasavi@marmara.edu.tr

Abbreviations Used

AUC = area under the curve
BP = biological process
CVD = cardiovascular disease
DDX52 = DEAD-box helicase 52
DEG = differentially expressed gene
DEmiRNA = differentially expressed miRNA
DGB = Drug Gene Budger
ESC/ERS = European Society of Cardiology/European Respiratory Society
ESF1 = nucleolar pre-rRNA processing protein
FC = fold-change
FDR = false discovery rate
GEO = Gene Expression Omnibus
GO = Gene Ontology
GS = gene significance
HDCA = histone deacetylase
HNRNPA3 = heterogeneous nuclear ribonucleoprotein A3
IPAH = idiopathic pulmonary arterial hypertension
IPF = idiopathic pulmonary fibrosis
KEGG = Kyoto Encyclopedia of Genes and Genomes
L100FWD = L1000 fireworks display
LIMMA = Linear Models of Microarray Data
ME = module eigengene
MM = module membership
PCC = Pearson correlation coefficient
PPI = protein-protein interaction
RFC1 = replication factor C subunit 1
ROC = receiver operating characteristic
RSRC1 = arginine and serine rich coiled coil 1
SEG = significantly expressed gene
TOM = topological overlap matrix
WGCNA = weighted gene coexpression network analysis